Published in final edited form as:
Free Radic Biol Med. 2013 December ; 65: 1201–1208. doi:10.1016/j.freeradbiomed.2013.09.008.

Mitochondrial glutathione depletion reveals a novel role for the pyruvate dehydrogenase complex as a key H_2O_2 emitting source under conditions of nutrient overload

Kelsey H. Fisher-Wellman[*,¥], **Laura A. A. Gilliam**[*,¥], **Chien-Te Lin**[*,¥], **Brook L. Cathey**[*,¥], **Daniel S. Lark**[*,^], and **P. Darrell Neufer**[*,^,¥]

[*]East Carolina Diabetes and Obesity Institute, East Carolina University, Greenville, NC, USA

[¥]Department of Physiology, East Carolina University, Greenville, NC, USA

[^]Department of Kinesiology, East Carolina University, Greenville, NC, USA

Abstract

Once regarded as "byproducts" of aerobic metabolism, the production of superoxide/H_2O_2 is now understood to be a highly specialized and extensively regulated process responsible for exerting control over a vast number of thiol-containing proteins, collectively referred to as the redox-sensitive proteome. Although disruptions within this process, secondary to elevated peroxide exposure, have been linked to disease, delineation of the sources and mechanisms regulating increased peroxide burden remain poorly defined and as such difficult to target using pharmacotherapy. Here we identify the pyruvate dehydrogenase complex (PDC) as a key source of H_2O_2 within skeletal muscle mitochondria under conditions of depressed glutathione redox buffering integrity. Treatment of permeabilized myofibers with varying concentrations of the glutathione depleting agent 1-chloro-2,4-dinitrobenzene (CDNB) led to a dose-dependent increase in pyruvate-supported JH_2O_2 emission, with emission rates eventually rising to exceed those of all substrate combinations tested. This striking sensitivity to glutathione depletion was observed in permeabilized fibers prepared from multiple species and was specific to PDC. Physiological oxidation of the cellular glutathione pool following high fat feeding in rodents was found to elevate PDC JH_2O_2 emission, as well as increase the sensitivity of the complex to GSH depletion. These findings reveal PDC as a potential major site of H_2O_2 production that is extremely sensitive to mitochondrial glutathione redox status.

Keywords

pyruvate dehydrogenase complex; mitochondria; skeletal muscle; reactive oxygen species; glutathione

INTRODUCTION

In mammalian mitochondria, currently identified sites of electron leak/superoxide ($O_2^{\bullet -}$) formation in the electron transport system (ETS) include the flavin mononucleotide and

Corresponding author: Kelsey H. Fisher-Wellman, PhD Department of Physiology, East Carolina University 500 Moye Boulevard Greenville, NC 27858 Phone: (252) 744-2760 Fax: (252) 744-3460 fisherwellmank@ecu.edu.

ubiquinone binding site within complex I, the quinone at centre "o" within complex III, the quinone binding site within glycerol-3-phosphate dehydrogenase, and the electron transferring flavoprotein Q oxioreductase [1]. In addition to the ETS, several non-respiratory chain sites of superoxide production have been identified including the matrix dehydrogenase enzyme complexes pyruvate dehydrogenase (PDC) and α-ketoglutarate dehydrogenase [2-4]. Mammalian PDC is comprised of three main catalytic components (E1-pyruvate dehydrogenase, E2- dihydrolipoyl transacetylase, E3-dihydrolipoamide dehydrogenase), which combine to form a large (~9.5 MDa) multi-subunit holoenzyme with a stoichiometry of 40:40:20 (E1:E2:E3) [5]. Experiments conducted using isolated enzyme have demonstrated PDC-stimulated rates of $O_2^{\bullet-}$ to be maximal under conditions in which the steady-state ratio of dihydrolipoate to lipoate within E2 is shifted in favor of the reduced form and supply of NAD+ is decreased (i.e., ↑dihydrolipate/lipoate, ↑NADH/NAD+). Under these conditions, it is believed that E3 catalyzes a $1e^-$ oxidation reaction between O_2 and E2-bound dihydrolipoate, in turn leading to either $O_2^{\bullet-}$ and/or a thiyl radical [3, 6]. While the isolated enzyme experiments demonstrate the potential of PDC to generate $O_2^{\bullet-}$, absolute rates H_2O_2 production (the dismutation product of $O_2^{\bullet-}$) by PDC and the α-ketoglutarate dehydrogenase complex within isolated mitochondria preps are typically much lower than that of succinate or palmitoyl-L-carnitine [1, 7], and thus the extent to which either enzyme contributes to H_2O_2 production in a physiological context has not been clear.

Regardless of the source, H_2O_2 produced is in turn degraded to H_2O by redox buffering networks comprised of glutathione and/or thioredoxin in conjunction with their associated enzymatic components (glutaredoxin, glutathione peroxidase, glutathione reductase and peroxiredoxin, thioredoxin reductase, respectively). The rate of H_2O_2 generation relative to flux throughout the redox buffering networks determines the redox status of cysteine containing proteins throughout the cell, thereby conferring regulation to various redox-sensitive cell processes [8, 9], including insulin sensitivity [10]. Interestingly, while redundancy exists within the system, there is evidence suggesting the glutathione and thioredoxin pathways act as independently regulated redox buffering networks [9]. In line with this notion, recent findings have identified a role for thioredoxin reductase in specifically regulating ETS-derived JH_2O_2 emission within cardiac and skeletal muscle mitochondria [11, 12].

The present study was designed to determine the influence of the glutathione redox buffering network on site-specific H_2O_2 production. Experiments conducted using permeabilized skeletal muscle fibers derived from multiple species (e.g., mice, rat and human) revealed a novel mechanism for glutathione in controlling PDC derived H_2O_2 emission. Specifically, pyruvate-supported H_2O_2 production by PDC was found to be remarkably sensitive to mitochondrial glutathione depletion, generating rates of H_2O_2 emission far greater than any other site/substrate combination tested. Oxidation of the cellular glutathione pool in response to high fat feeding was subsequently shown to elevate pyruvate-supported JH_2O_2 emission within skeletal muscle, as well as increase the sensitivity of PDC to glutathione depletion. To our knowledge this is the first evidence that PDC is capable of generating substantial rates of H_2O_2 production and thus could potentially represent a major source for mitochondrial derived H_2O_2 within skeletal muscle, especially in response to nutrient overload or other conditions in which the mitochondrial glutathione pool has undergone a shift to a more oxidized state (e.g., metabolic disease).

METHODS

Animals and Reagents

All animal studies were approved by the East Carolina University Institutional Animal Care and Use Committee, which is in accordance with international regulations. C57BL/6NJ mice

(~ 10 weeks old) were purchased from Jackson Laboratory. Male Sprague-Dawley rats (12-16 weeks old) were purchased from Charles River Laboratory. All rodents were housed in a temperature (22°C) and light controlled (12 hour light/12 hour dark) room and maintained on a standard chow diet with free access to food and water. For the high fat diet (HFD) study, a subset of rats were switched to a 60% lard based HFD (Research Diets Inc., Product # D12492) for a period of 6 weeks. For all experiments, rodents were fasted 4 hours, anesthetized, and red and white portions of the gastrocnemius muscle were dissected and separated into fiber bundles. Remaining portions of muscle were frozen (liquid N_2) for later analysis. All reagents and chemicals were obtained from Sigma-Aldrich (including PDC from porcine heart) with the exception of Amplex Ultra Red reagent (Invitrogen).

Preparation of permeabilized fiber bundles

This technique is partially adapted from previous methods and has been thoroughly described [13]. For experiments involving GSH depletion, 1-chloro-2,4-dinitrobenzene (CDNB) or ethanol was added during saponin permeabilization. Following permeabilization, fibers were washed in ice-cold wash buffer [K-MES (110 mM), KCl (35 mM), EGTA (1 mM), K_2HPO_4 (5 mM), $MgCl_2$-6H2O (3 mM), BSA (0.5mg/ml) pH 7.1, 295 mOsm) to remove endogenous substrates and un-reacted CDNB. This method has previously been shown using isolated mitochondria to prevent direct CDNB-derived superoxide generation [14]. Washout of residual CDNB was also necessary to prevent interference with the Amplex Ultra Red/ horseradish peroxidase detection system (data not shown); washout was confirmed by lack of an increase in resorufin fluorescence during glutamate/malate energized conditions.

Mitochondrial respiration and H_2O_2 emission measurements

High-resolution O_2 consumption measurements were conducted at 37°C in wash buffer, supplemented with creatine monohydrate (25 mM), using the OROBOROS O_2K Oxygraph. Mitochondrial H_2O_2 emission was measured fluorometrically at 37°C via Amplex Ultra Red (10 μM) / horseradish peroxidase (3 U/ml) detection system (Ex:Em 565:600). Fluorescence was monitored using a SPEX Fluoromax 3 (HORIBA Jobin Yvon) spectrofluorometer with temperature control and magnetic stirring. For each experiment, resorufin fluorescence was converted to nM H_2O_2 via an H_2O_2 standard curve (Figure 1A & 1B) generated under identical substrate conditions (with the exception of a permeabilized fiber) as employed for each protocol. To this end, all substrates utilized were tested for any potential interference with the Amplex Ultra Red/ horseradish peroxidase detection system (Figure 1C). Blebbistatin (25 μM) was present during all O_2 consumption and H_2O_2 emission experiments to prevent contraction of the myofibers [13]. At the conclusion of each experiment, fiber bundles were washed in double-distilled H_2O to remove salts and freeze-dried in a lyophilizer (Lab-conco). The rate of respiration was expressed as pmol/s/mg dry weight and H_2O_2 emission as pmol/min/mg dry weight. The term JH_2O_2 emission represents the flux of H_2O_2 diffusing out of the mitochondrial matrix into the surrounding assay media, reflecting the balance between H_2O_2 production and scavenging in the matrix. The Amplex Ultra Red /horseradish peroxidase detection system is not capable of diffusing into the matrix where it could in theory react directly with H_2O_2 immediately upon production.

Mitochondrial NADH production

All NADH production assays were carried out in a potassium phosphate based buffer (50 mM), containing $CaCl_2$ (10 μM) and $MgCl_2$ (200 μM), pH 7.4. Permeabilized fibers were prepared as indicated above. Following a 15 minute wash in buffer Z, fibers were incubated with the pore-forming peptide alamethicin (30 μg/ml) to permeabilize the inner

mitochondrial membrane [2, 15]. Experiments were carried out in the presence of coenzyme A (100 μM), NAD^+ (1 mM), thiamine pyrophosphate (300 μM), rotenone (2 μM) and pyruvate (1 mM). NADH production was tracked via auto-fluorescence (Ex:Em 376/450). Fluorescence values were converted to μM NADH via an NADH standard curve.

Isolated PDC experiments

All experiments were carried out using PDC from porcine heart (Sigma-Aldrich) in potassium phosphate buffer described above with the addition of coenzyme A (100 μM) and thiamine pyrophosphate (300 μM). The enzyme concentration for all assays was 16.8 mU/ml. For H_2O_2 production experiments, buffer was supplemented with Amplex Ultra Red (10 μM) and horseradish peroxidase (3 U/ml). The term H_2O_2 production was used for all experiments involving isolated PDC, reflecting the absence of a scavenging system and direct detection by the Amplex Ultra Red/horseradish peroxidase . Coenzyme A was found to increase fluorescence; thus all H_2O_2 production experiments were performed after an 8 minute recording of fluorescence in the absence of substrate. Coenzyme A-induced fluorescence was subtracted out prior to data analysis. NADH production was assessed as stated above. Data are expressed as pmol/s/U.

GSH, GSSG, GSH/GSSG measurements

Frozen muscles were homogenized in TE buffer (10 mM Tris, 1 mM EDTA, pH 7.1) pre-bubbled with N_2 gas for ~20 minutes prior to homogenization. Pre-bubbling of buffer with N2 gas was shown to be critical for the prevention of ex-vivo oxidation of the glutathione pool, which over-estimates the concentration of GSSG (data not shown). Immediately following homogenization, a portion of homogenate was transferred to a separate tube containing 0.5 mM 1-methyl-2-vinylpyridinium triflate (M2VP), which alkylates all reduced GSH. The M2VP-treated sample was utilized to assess GSSG. Both the original sample and the sample treated with M2VP were subsequently centrifuged (10,000 RPM, 4°C) and supernatant was used to measure GSH and GSSG using the reagents and calibration set provided by the GSH/GSSG assay kit (Percipio Biosciences, Cat# 21040).

Human subjects and tissue biopsy

Three men and 2 women were recruited to participate in this investigation (age 26.2 ± 6.1, BMI 25.2 ± 3.7). None of the subjects had any disease or were taking medications known to alter metabolism. Subjects were given both oral and written information about the experimental procedures before giving their informed consent. The experiments were approved by the Institutional Review Board of East Carolina University and conducted in accordance with the Declaration of Helsinki principles. On the day of the experiment, subjects reported to the laboratory following an overnight fast (12 hours). Skeletal muscle biopsies were obtained from the lateral aspect of the vastus lateralis by the percutaneous needle biopsy technique under local subcutaneous anesthesia (1% lidocaine) and used to prepare permeabilized fiber bundles.

Statistics

Data are presented as mean ± SEM. Statistical analysis were performed using t-tests or 1-way ANOVA with Student-Newman-Keuls methods for analysis of significance among groups. The level of significance was set at $P < 0.05$.

RESULTS

Site-specific H_2O_2 emission: Effects of GSH depletion

To directly compare rates of electron leak from known sites within mitochondria, H_2O_2 emission was monitored in mouse permeabilized skeletal muscle fiber bundles under a variety of substrate combinations. As expected [16, 17], succinate, which feeds electrons directly into the Q-pool and induces reverse electron flow back into complex I, generated H_2O_2 emission rates higher than all other substrate combinations tested. Surprisingly however, pyruvate alone (i.e., no malate) also generated a substantial rate of H_2O_2 emission (Figure 2A).

To determine the impact of an oxidative shift in the mitochondrial redox environment on H_2O_2 emitting potential, permeabilized fiber bundles were pre-treated with the glutathione-depleting agent CDNB. Catalyzed by glutathione S-transferase, CDNB forms an irreversible conjugate with GSH, resulting in a gradual depletion of GSH [14, 18]. Treatment of permeabilized fibers with varying concentrations of CDNB led to a dose-dependent decrease in GSH (Figure 2B). Compared to GSH-replete fibers, partial depletion (1 μM CDNB; ~75% of control) of GSH did not significantly increase H_2O_2 emission when fibers were energized with glutamate/malate, palmitoyl-L-carnitine, α-ketoglutarate, glycerol-3-phosphate, or succinate (Figure 2D). In stark contrast, when respiration was supported solely by pyruvate, H_2O_2 emission rate increased by more than 20-fold (13.2 ± 1.4 (Fig 2A) vs 281.2 ± 26.8 (Fig 2D) pmol/min/mg dry wt). These rates were higher than all other substrate combinations, including succinate (Figure 2C).

Mitochondrial redox buffering networks are comprised of both the glutathione and thioredoxin systems. To determine the specificity of the pyruvate response to GSH depletion, experiments were repeated in the presence of inhibitors of glutathione reductase (bis-chloroethylnitrosourea, BCNU) or thioredoxin reductase (auranofin, AF) without depleting matrix GSH. Under these conditions, both BCNU and AF increased pyruvate-supported JH_2O_2 emission (Figure 2E & 2F), but the effect was marginal relative to GSH depletion, thus suggesting direct control of PDC by glutathione. Adding the inhibitors in the reverse order did not affect the results (data not shown). In an attempt to rescue the effect of CDNB exposure observed under pyruvateenergized conditions, CDNB-treated fibers were subjected to an additional 15 minute incubation in wash buffer supplemented with 25 mM GSH prior to JH_2O_2 assessment. Pre-incubation in GSH only partially restored emission rates to that of control (i.e., GSH-replete) fibers (Figure 2G). Interestingly, the elevated JH_2O_2 emission following GSH depletion occurred in the absence of any change in pyruvate-supported NADH production (non-ADP stimulated; Figure 2H) or respiratory kinetics during both non-ADP and ADP-stimulated respiration (Figure 2I).

Inter-species susceptibility of PDC-mediated H_2O_2 emission to GSH depletion

To determine if pyruvate-supported H_2O_2 emission was responsive to more physiological declines in GSH, rates of H_2O_2 emission were assessed in permeabilized mouse skeletal muscle fiber bundles pre-treated with varying concentrations of CDNB. As little as ~6% depletion in GSH generated a significant increase in pyruvate-supported H_2O_2 emission, with values rising exponentially as GSH levels continued to fall (Figure 3A). This striking sensitivity to GSH depletion was also evident in permeabilized fiber bundles prepared from rats (Figure 3B) and humans (Figure 3C). Interestingly, higher concentrations of CDNB were required in rat and human fibers to induce a comparable level of GSH depletion as that seen in mice, possibly reflecting inter-species differences in total GSH content and/or glutathione-S-transferase expression/activity.

PDC generates H_2O_2 directly at a rate responsive to NADH/NAD and is primarily independent of mitochondrial membrane potential

With respect to the source of H_2O_2 under pyruvate energized conditions, previous studies have identified direct production of H_2O_2 from the dihydrolipoyl dehydrogenase component of PDC [19, 20]. Moreover, H_2O_2 generation independent of mitochondrial membrane potential has also been reported by the closely associated α-ketoglutarate dehydrogenase complex [2, 6]. To investigate the mechanisms regulating H_2O_2 production in relation to catalytic flux, a series of experiments were carried out using isolated PDC. In agreement with previous findings [2, 6] isolated PDC was found to generate substantial rates of H_2O_2 in the presence of pyruvate (Figure 4A). Exogenous superoxide dismutase (SOD) was included in the preceding experiment to ensure superoxide produced by PDC was converted to H_2O_2. Surprisingly, omission of SOD did not affect pyruvate-supported H_2O_2 production (Figure 4B) whereas inclusion of catalase eliminated the signal (Figure 4C), suggesting PDC was producing H_2O_2 directly. This is not without precedent as certain isoforms of NADPH oxidase [21] and xanthine oxidase [22] have also been shown to generate H_2O_2 directly.

To determine the influence of NADH/NAD+ on PDC-supported JH_2O_2, experiments were conducted in response to increasing concentrations of pyruvate either in the absence or presence of NAD^+. In the absence of NAD^+, PDC JH_2O_2 production was extremely sensitive to the concentration of pyruvate (i.e., pseudo K_m < 1 μM pyruvate) whereas in the presence of NAD^+ the pseudo Km for pyruvate increased by greater than 60-fold (Figure 4D & 4E). Under physiological conditions, the ratio of NADH/NAD^+ varies as a function of metabolic balance. To assess the influence of dynamic fluctuations in NADH/NAD^+ on PDC-mediated H_2O_2 generation, pyruvate-supported *J*NADH and JH_2O_2 were monitored in parallel under identical substrate conditions. The starting NAD^+ concentration for these assays was 50 μM (~K_m for *J*NADH; data not shown). Upon addition of pyruvate (1 mM), NAD^+ was rapidly converted to NADH (Figure 4F, grey trace), gradually leveling off after ~10 min at a maximum concentration of ~28 μM and a ratio of NADH/NAD^+ slightly >1. By contrast, the rate of H_2O_2 production by PDC appeared to increase in direct proportion to the rise in NADH (Figure 4F, black trace). When the H_2O_2/NADH values for both readouts were converted to point by point production rates, the flux derivations were near mirror images of one another (Figure 4G), consistent with the notion that NAD^+-mediated re-oxidation of E2-bound dihydrolipoate is a critical determinant of PDC-mediated H_2O_2 production.

To determine if pyruvate-supported JH_2O_2 emission was indeed originating from PDC and not the ETS within an intact system (i.e., permeabilized fiber), JH_2O_2 emission experiments were carried out in the absence and presence of the chemical uncoupler trifluorocarbonylcyanide phenylhydrazone (FCCP) or maximal ADP. Addition of FCCP, which maximizes proton conductance and dissipates the membrane potential, eliminated ETS-derived H_2O_2 emission (Figure 4H, Succ). In contrast, FCCP only marginally depressed pyruvate-supported JH_2O_2 emission in fibers pre-treated with 100 nM CDNB (Figure 4H, Pyr+CDNB). In support of these findings, pyruvate-supported JH_2O_2 emission was not depressed in the presence of maximal ADP following pre-treatment with varying concentrations of CDNB (Figure 4I). Taken together, these findings suggest the PDC complex is the source of H_2O_2 under pyruvate-energized conditions.

High fat feeding induces an oxidative shift in glutathione redox poise and elevates pyruvate-supported JH_2O_2 emission

The level of decrease in GSH necessary to trigger an increase in PDC-supported H_2O_2 emission (~20% depletion) has been observed in a variety of pathological conditions thought to have a reactive oxygen species-mediated component in their etiology [23-26]. Therefore,

it was hypothesized that high fat feeding may increase the sensitivity of PDC to GSH depletion, thus elevating the peroxide burden imposed in the presence of pyruvate. To test this hypothesis, rats were placed on a 60% HFD for a period of 6 weeks. Consistent with previous reports [25, 26], high fat feeding resulted in an oxidation of the cellular glutathione pool within skeletal muscle (Figure 5A). It should be noted that the GSH/GSSG redox state assay was performed on whole skeletal muscle homogenate and thus does not provide information related to compartment (e.g., mitochondria, endoplasmic reticulum, cytosol) specific effects of the HFD on GSH/GSSG redox posie. To determine if the HFD-induced oxidative shift in overall glutathione redox poise was sufficient to elevate pyruvate-supported JH_2O_2 emission, permeabilized fiber bundles were prepared from red and white gastrocnemius muscle of chow and high fat fed rats and pre-treated with varying concentrations of CDNB. In red gastrocnemius muscle, pyruvate-supported JH_2O_2 emission was higher in the fibers prepared from high fat fed rats under control (0 nM CDNB) conditions, as well as in fibers exposed to increasing concentrations of CDNB (Figure 5B). Similar results were evident when these experiments were repeated in fibers prepared from white gastrocnemius muscle (Figure 5C). Succinate supported JH_2O_2 emission was also found to be higher in the high fat fed rats (Figure 5D). Similar to that observed in Figure 2A, succinate-supported JH_2O_2 emission was relatively unaffected by CDNB exposure. Assessment of pyruvate-supported respiratory kinetics did not reveal any differences in respiration between chow and high fat fed rats (Figure 5E & 5F).

DISCUSSION

The present findings reveal PDC as a pivotal sensor and regulator within the redox circuitry system that integrates with the glutathione redox buffering network to regulate H_2O_2 production. In this context, there are three main findings from the present study. First, PDC was shown to generate H_2O_2 as a function of matrix GSH content, with recorded emission rates in GSH-depleted fibers exceeding those of any other substrate combination tested. This dramatic sensitivity of PDC to declines in matrix GSH content was particularly interesting in that the effect was unique to PDC alone, as it did not occur under any other substrate combinations. Second, isolated PDC was found to generate H_2O_2 directly at a rate responsive to NADH/NAD^+. Moreover, JH_2O_2 emission experiments conducted using permeabilized fibers in the presence of FCCP and ADP revealed PDC-mediated H_2O_2 production to be independent of mitochondrial membrane potential. Lastly, physiological oxidation of the cellular glutathione pool via high fat feeding was found to increase pyruvate-supported JH_2O_2 emission, as well as increase the sensitivity of PDC to GSH loss within permeabilized myofibers. To our knowledge, this is the first evidence demonstrating a role for matrix glutathione in regulating PDC H_2O_2 production. Collectively, these findings reveal an extremely sensitive and exquisitely balanced network between PDC and the glutathione redox buffering network that both senses and responds to reducing pressure in accordance with the overall state of the mitochondrial redox environment. This supports a novel paradigm, exemplified by PDC, in which control of the redox environment is exerted and dominated by the redox buffering network rather than simply production of reactive oxygen species.

The dependence of PDC-derived H_2O_2 on matrix GSH content is a novel finding, as no other site was found to respond in a similar fashion, including the α-ketoglutarate dehydrogenase complex which is quite similar structurally to PDC. The level of decrease in GSH necessary to trigger an increase in H_2O_2 emission (~6-25% depletion) is observed in a variety of pathological conditions, including diet-induced insulin resistance, diabetes, and aging [23-26]. The dependence of PDC-derived H_2O_2 on GSH appears to be specific to the glutathione molecule itself rather than a redox buffering enzyme-coupled system, as inhibition of glutathione reductase or thioredoxin reductase in the absence of GSH depletion

only modestly increased pyruvate-supported H_2O_2 emission. It is possible that depletion of GSH led to an inactivation of glutathione peroxidase and a subsequent increase in H_2O_2 emission. However, given that glutathione peroxidase works in conjunction with glutathione reductase [9], the lack of a robust increase in pyruvate-supported H_2O_2 emission in the presence of BCNU suggests a minimal role for glutathione peroxidase in regulating PDC H_2O_2 production. These findings therefore imply the existence of some form of direct GSH-mediated scavenging and/or physical association of glutathione with PDC. With respect to the latter, the E2-bound lipoyl moieties within PDC are prime targets for glutathionylation, and indirect evidence for both reversible glutathionylation of the lipoyl groups bound to E2 in the α-ketoglutarate dehydrogenase complex [27], as well as direct interaction with thioredoxin and glutathione [3], have been reported. However, using a direct immunoblotting approach [28, 29], we were unable to detect glutathionylation of the E2 component of PDC under several different experimental conditions (data not shown), supporting the former notion that GSH is functioning as a direct scavenger of H_2O_2 within the complex. In this context, it is intriguing to consider the possibility that the high abundance of E2-bound lipoyl groups (3/E2 x 40 E2 = 120/PDC) may provide a source of reducing power to directly regenerate GSH from GSSG, creating an internal redox buffering circuit to counterbalance H_2O_2 production by the complex. Such a mechanism could also protect against irreversible inactivation of E1 by lipoate thiyl radicals that form when the complex is under elevated reducing pressure, a self-regulatory mechanism that has been observed in the α-ketoglutarate dehydrogenase complex [3, 6].

In the present investigation, PDC generated H_2O_2 independent of mitochondrial membrane potential. The dependence/independence on membrane potential is difficult to investigate in an intact system. Because there is no specific, membrane-permeable inhibitor of NADH oxidation at complex I, the source of H_2O_2 for all experiments using permeabilized fibers has to be interpreted in the context of the ETS. Moreover, use of any ETS inhibitor (e.g., rotenone, antimycin A, cyanide) to isolate the impact of PDC will in turn lead to an increase in NADH/NAD^+ which will affect PDC-H_2O_2 generation [2]. Indirect evidence for PDC as the primary source of H_2O_2 during pyruvate-stimulated conditions was provided by comparing the impact of FCCP and ADP between pyruvate and succinate energized conditions. Succinate-supported H_2O_2 arises from the ETS, with the exception of a small contribution from the flavin moiety of succinate dehydrogenase [30], and is highly dependent on mitochondrial membrane potential. Succinate supported H_2O_2 was completely absent in the presence of FCCP, confirming the dependence on mitochondrial membrane potential. By contrast, pyruvate-stimulated H_2O_2 was relatively unaffected by FCCP and was surprisingly elevated under maximal ADP stimulated conditions. Taken together, these findings suggest that matrix dehydrogenases (e.g., PDC and the α-ketoglutarate dehydrogenase complex) are likely continual sources of H_2O_2 within skeletal muscle mitochondria, the potential being greatest for PDC due to its sensitivity to the glutathione redox buffering network.

In aggregate, the current study demonstrates a role for PDC as a key H_2O_2 emitting source under conditions of compromised glutathione redox buffering integrity. Under normal conditions, the glutathione redox buffering network masks the majority of H_2O_2 arising from PDC. However, loss of GSH and/or oxidation of the GSH/GSSG redox couple accelerate PDC-derived H_2O_2. Based on this notion, the most likely metabolic states which would be expected to favor maximal levels of H_2O_2 emission from PDC include those in which pyruvate availability is high (e.g., post-prandial), and when matrix GSH/GSSG has undergone an oxidative shift. Oxidation of the GSH/GSSG redox couple has been reported in a variety of chronic pathophysiological states, including, aging, diabetes and obesity-induced insulin resistance [23-26], as well as under even more acute (4 h) high dietary fat overload states in humans [25]. Given the relatively large size of PDC (~9.5 MDa) in

conjunction with its striking sensitivity to GSH depletion, it is possible that PDC-supported H_2O_2 functions as a type of mitochondrial-derived signal emitted under conditions of positive metabolic balance designed to counterbalance the elevated reducing pressure stemming from excess nutrients. To place in a physiological context, the implication is that conditions in which the matrix GSH/GSSG redox couple and/or total GSH content are reduced due to nutrient overload (e.g., high fat diet) [25], aging or disease [23, 24], will generate a net increase in H_2O_2 emission for a given degree of PDC flux.

Acknowledgments

This work was supported by funding from the NIH; 1F32AR061946 (LAAG), 1R01DK074825 and 1R01096907 (P.D.N.).

REFERENCES

1. Brand MD. The sites and topology of mitochondrial superoxide production. Exp Gerontol. 2010; 45:466–472. [PubMed: 20064600]
2. Starkov AA, Fiskum G, Chinopoulos C, Lorenzo BJ, Browne SE, Patel MS, Beal MF. Mitochondrial alpha-ketoglutarate dehydrogenase complex generates reactive oxygen species. J Neurosci. 2004; 24:7779–7788. [PubMed: 15356189]
3. Bunik VI. 2-Oxo acid dehydrogenase complexes in redox regulation. Eur J Biochem. 2003; 270:1036–1042. [PubMed: 12631263]
4. Tretter L, Adam-Vizi V. Generation of reactive oxygen species in the reaction catalyzed by alpha-ketoglutarate dehydrogenase. J Neurosci. 2004; 24:7771–7778. [PubMed: 15356188]
5. Brautigam CA, Wynn RM, Chuang JL, Chuang DT. Subunit and catalytic component stoichiometries of an in vitro reconstituted human pyruvate dehydrogenase complex. J Biol Chem. 2009; 284:13086–13098. [PubMed: 19240034]
6. Bunik VI, Sievers C. Inactivation of the 2-oxo acid dehydrogenase complexes upon generation of intrinsic radical species. Eur J Biochem. 2002; 269:5004–5015. [PubMed: 12383259]
7. Rindler PM, Plafker SM, Szweda LI, Kinter M. High dietary fat selectively increases catalase expression within cardiac mitochondria. J Biol Chem. 2013; 288:1979–1990. [PubMed: 23204527]
8. Jones DP, Go YM. Mapping the cysteine proteome: analysis of redox-sensing thiols. Curr Opin Chem Biol. 2010
9. Adimora NJ, Jones DP, Kemp ML. A model of redox kinetics implicates the thiol proteome in cellular hydrogen peroxide responses. Antioxid Redox Signal. 2010; 13:731–743. [PubMed: 20121341]
10. Fisher-Wellman KH, Neufer PD. Linking mitochondrial bioenergetics to insulin resistance via redox biology. Trends Endocrinol Metab. 2012; 23:142–153. [PubMed: 22305519]
11. Fisher-Wellman KH, Mattox TA, Thayne K, Katunga LA, La Favor JD, Neufer PD, Hickner RC, Wingard CJ, Anderson EJ. Novel role for thioredoxin reductase-2 in mitochondrial redox adaptations to obesogenic diet and exercise in heart and skeletal muscle. J Physiol. 2013; 591:3471–3486. [PubMed: 23613536]
12. Stanley BA, Sivakumaran V, Shi S, McDonald I, Lloyd D, Watson WH, Aon MA, Paolocci N. Thioredoxin reductase-2 is essential for keeping low levels of H(2)O(2) emission from isolated heart mitochondria. J Biol Chem. 2011; 286:33669–33677. [PubMed: 21832082]
13. Perry CG, Kane DA, Lin CT, Kozy R, Cathey BL, Lark DS, Kane CL, Brophy PM, Gavin TP, Anderson EJ, Neufer PD. Inhibiting myosin-ATPase reveals a dynamic range of mitochondrial respiratory control in skeletal muscle. Biochem J. 2011; 437:215–222. [PubMed: 21554250]
14. Treberg JR, Quinlan CL, Brand MD. Hydrogen peroxide efflux from muscle mitochondria underestimates matrix superoxide production--a correction using glutathione depletion. FEBS J. 2010; 277:2766–2778. [PubMed: 20491900]
15. Gostimskaya IS, Grivennikova VG, Zharova TV, Bakeeva LE, Vinogradov AD. In situ assay of the intramitochondrial enzymes: use of alamethicin for permeabilization of mitochondria. Anal Biochem. 2003; 313:46–52. [PubMed: 12576057]

16. St-Pierre J, Buckingham JA, Roebuck SJ, Brand MD. Topology of superoxide production from different sites in the mitochondrial electron transport chain. The Journal of biological chemistry. 2002; 277:44784–44790. [PubMed: 12237311]

17. Anderson EJ, Neufer PD. Type II skeletal myofibers possess unique properties that potentiate mitochondrial H(2)O(2) generation. Am J Physiol Cell Physiol. 2006; 290:C844–851. [PubMed: 16251473]

18. Han D, Canali R, Rettori D, Kaplowitz N. Effect of glutathione depletion on sites and topology of superoxide and hydrogen peroxide production in mitochondria. Mol Pharmacol. 2003; 64:1136–1144. [PubMed: 14573763]

19. Tahara EB, Barros MH, Oliveira GA, Netto LE, Kowaltowski AJ. Dihydrolipoyl dehydrogenase as a source of reactive oxygen species inhibited by caloric restriction and involved in Saccharomyces cerevisiae aging. FASEB J. 2007; 21:274–283. [PubMed: 17110466]

20. Kareyeva AV, Grivennikova VG, Vinogradov AD. Mitochondrial hydrogen peroxide production as determined by the pyridine nucleotide pool and its redox state. Biochim Biophys Acta. 2012; 1817:1879–1885. [PubMed: 22503830]

21. Leto TL, Morand S, Hurt D, Ueyama T. Targeting and regulation of reactive oxygen species generation by Nox family NADPH oxidases. Antioxid Redox Signal. 2009; 11:2607–2619. [PubMed: 19438290]

22. Kelley EE, Khoo NK, Hundley NJ, Malik UZ, Freeman BA, Tarpey MM. Hydrogen peroxide is the major oxidant product of xanthine oxidase. Free radical biology & medicine. 2010; 48:493–498. [PubMed: 19941951]

23. Sekhar RV, Patel SG, Guthikonda AP, Reid M, Balasubramanyam A, Taffet GE, Jahoor F. Deficient synthesis of glutathione underlies oxidative stress in aging and can be corrected by dietary cysteine and glycine supplementation. Am J Clin Nutr. 2011; 94:847–853. [PubMed: 21795440]

24. Sekhar RV, McKay SV, Patel SG, Guthikonda AP, Reddy VT, Balasubramanyam A, Jahoor F. Glutathione synthesis is diminished in patients with uncontrolled diabetes and restored by dietary supplementation with cysteine and glycine. Diabetes Care. 2011; 34:162–167. [PubMed: 20929994]

25. Anderson EJ, Lustig ME, Boyle KE, Woodlief TL, Kane DA, Lin CT, Price JW 3rd, Kang L, Rabinovitch PS, Szeto HH, Houmard JA, Cortright RN, Wasserman DH, Neufer PD. Mitochondrial H2O2 emission and cellular redox state link excess fat intake to insulin resistance in both rodents and humans. The Journal of clinical investigation. 2009; 119:573–581. [PubMed: 19188683]

26. Ritchie IR, Dyck DJ. Rapid loss of adiponectin-stimulated fatty acid oxidation in skeletal muscle of rats fed a high fat diet is not due to altered muscle redox state. PLoS One. 2012; 7:e52193. [PubMed: 23284930]

27. Applegate MA, Humphries KM, Szweda LI. Reversible inhibition of alpha-ketoglutarate dehydrogenase by hydrogen peroxide: glutathionylation and protection of lipoic acid. Biochemistry. 2008; 47:473–478. [PubMed: 18081316]

28. Kang PT, Zhang L, Chen CL, Chen J, Green KB, Chen YR. Protein thiyl radical mediates S-glutathionylation of complex I. Free Radic Biol Med. 2012; 53:962–973. [PubMed: 22634394]

29. Chen CA, Wang TY, Varadharaj S, Reyes LA, Hemann C, Talukder MA, Chen YR, Druhan LJ, Zweier JL. S-glutathionylation uncouples eNOS and regulates its cellular and vascular function. Nature. 2010; 468:1115–1118. [PubMed: 21179168]

30. Quinlan CL, Orr AL, Perevoshchikova IV, Treberg JR, Ackrell BA, Brand MD. Mitochondrial complex II can generate reactive oxygen species at high rates in both the forward and reverse reactions. J Biol Chem. 2012; 287:27255–27264. [PubMed: 22689576]

HIGHLIGHTS

- Matrix GSH depletion reveals PDC as a major source of H_2O_2 production.
- PDC generates H_2O_2 directly, independent of mitochondrial membrane potential.
- High fat feeding oxidizes cellular GSH and elevates PDC-mediated JH_2O_2 emission.

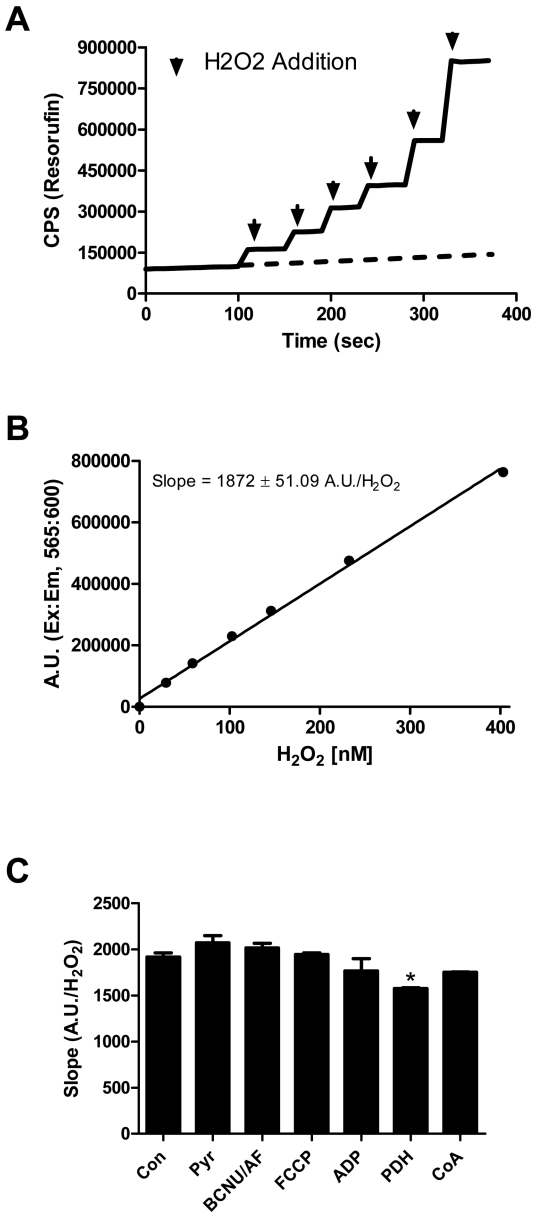

Figure 1. Detection of H_2O_2 via Amplex Ultra Red and Horse radish peroxidase

(**A**) Representative trace of an H_2O_2 standard curve experiment. Black arrows indicate the addition of H_2O_2. To correct for the increase in background fluorescence of the Amplex Ultra Red/HRP detection system over time, fluorescence was monitored for a period of ~8-10 minutes during each experiment prior to H_2O_2/substrate addition (background fluorescence extrapolated as dotted line). This background rate of fluorescence was then subtracted from each resorufin trace prior to slope and Y-intercept calculation (for standard curve experiments) or conversion to nM H_2O_2 (H_2O_2 emission experiments). (**B**) Representative H_2O_2 standard curve. (**C**) Quantified slopes (resorufin A.U./H_2O_2) from H_2O_2 standard curve experiments performed in the presence of various substrates. * Different from Con ($p < 0.05$). Data are mean ± SEM ($n = 3$).

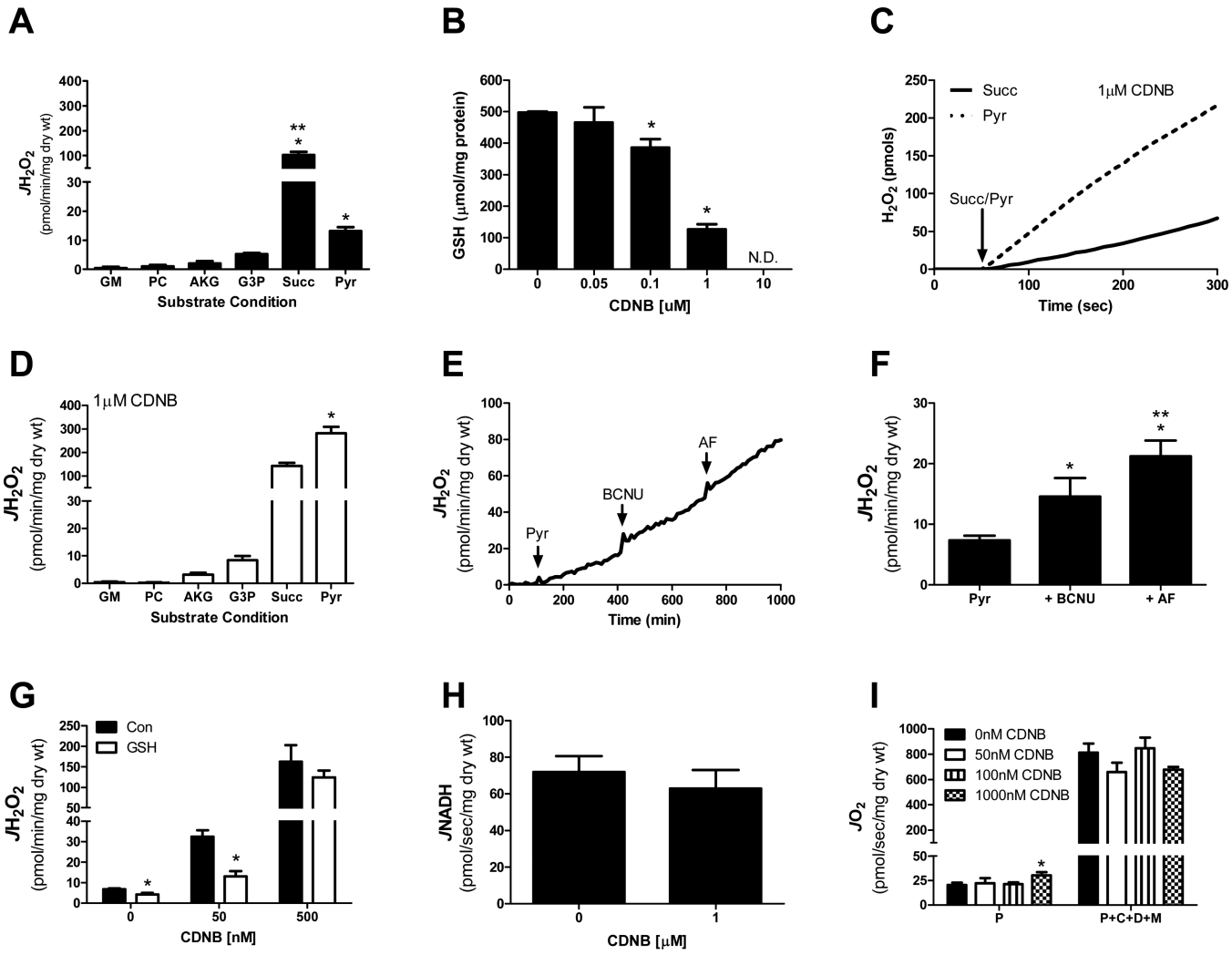

Figure 2. Glutathione depletion elevates pyruvate-supported JH_2O_2 emission within permeabilized myofibers

Permeabilized fibers were prepared from RG of C57BL/6N mice (**A-I**). H_2O_2 emission rate (JH_2O_2) was assessed in response to glutamate-malate (GM 10 mM-2 mM), palmitoyl-carnitine (PC 25 μM), α-ketoglutarate (AKG 10 mM), glycerol-3-phosphate (G3P 10 mM), succinate (Succ 10 mM), pyruvate (Pyr 1 mM). * Different from GM, PC, AKG, G3P ($p < 0.05$). **Different from all other substrate combinations ($p < 0.05$). (**B**) GSH was assessed in fibers pre-treated with varying concentrations of CDNB. *Different from 0 μM condition ($p < 0.05$). (**C**) Representative H_2O_2 emission experiment in response to pyruvate (1 mM) or succinate (10 mM) in fibers pre-treated with 1 μM CDNB (dry weights of fibers for each experiment were within 0.01 mg). (**D**) Quantified rates (CDNB effect) from experiment depicted in panel C, as well as the remaining substrate combinations. *Higher than all other substrate combinations ($p < 0.05$). (**E**) Representative H_2O_2 emission experiment in response to pyruvate (1 mM), BCNU (100 μM), AF (1μM) in control fibers. (**F**) Quantified rates from experiment depicted in panel E. *Different from Pyr ($p < 0.05$), **Different from + BCNU ($p < 0.05$). (**G**) Fibers were pre-treated with 0, 50, or 500nM CDNB, following by a 15 minute wash in the absence or presence of 25 mM GSH. Pyruvate (1 mM) supported H_2O_2 emission was then assessed. * Different from Con ($p < 0.05$). (**H**) Pyruvate-supported NADH production in fibers pre-treated with 0 or 1000 nM CDNB. (**I**) JO_2 consumption was

assessed in fibers pre-treated with 0, 50, 100 or 1000nM CDNB. Substrate conditions included pyruvate alone (P; 1 mM) and Pyruvate+Carnitine+ADP+malate (P+C+D+M 1/5/2/5 mM). *Different from 0 nM condition ($p < 0.05$). Data are mean ± SEM, n = 4-7/group.

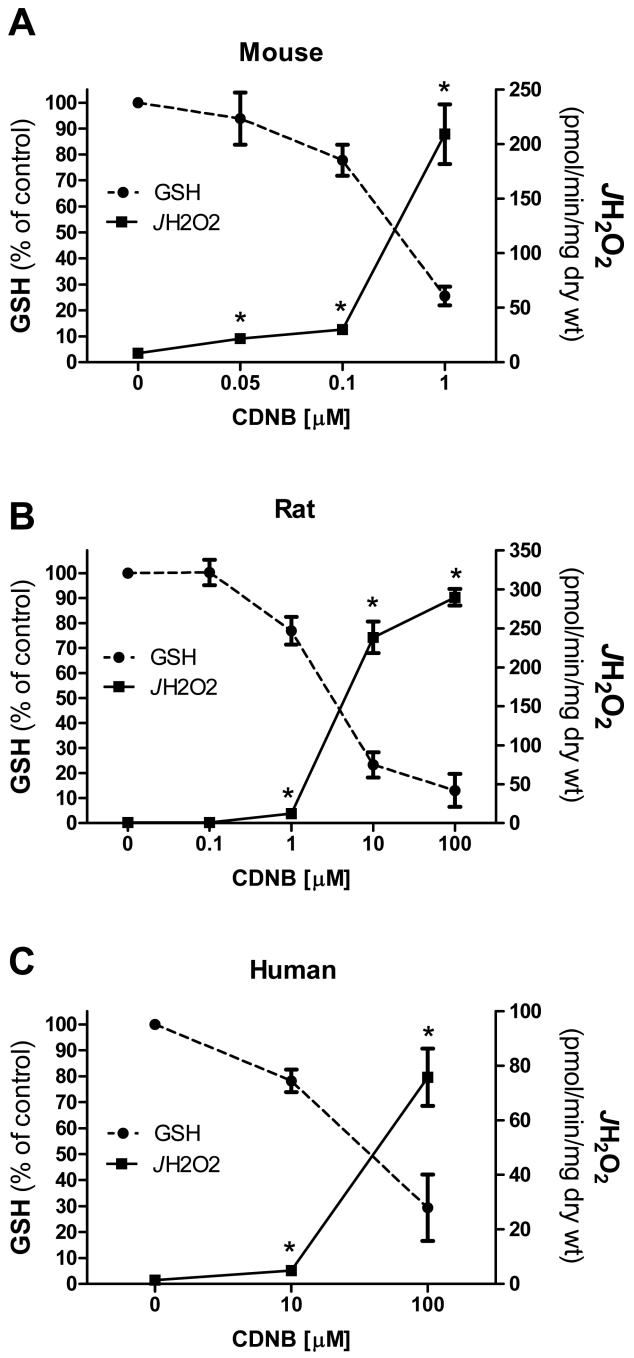

Figure 3. Sensitivity of pyruvate-supported JH_2O_2 to GSH depletion across species

Permeabilized fiber bundles were prepared from RG muscle of C57BL/6N mice (**A**), Sprague Dawley rats (**B**) or vastus lateralis muscle of human subjects (**C**). Fibers were pre-treated with varying concentrations of CDNB and pyruvate [1mM] supported H_2O_2 emission was then assessed. GSH was assessed as described in figure 2B for each species. Data are presented as % change from ethanol control. *Different from 0μM condition ($p < 0.05$). Data are mean ± SEM, n = 4-6/group.

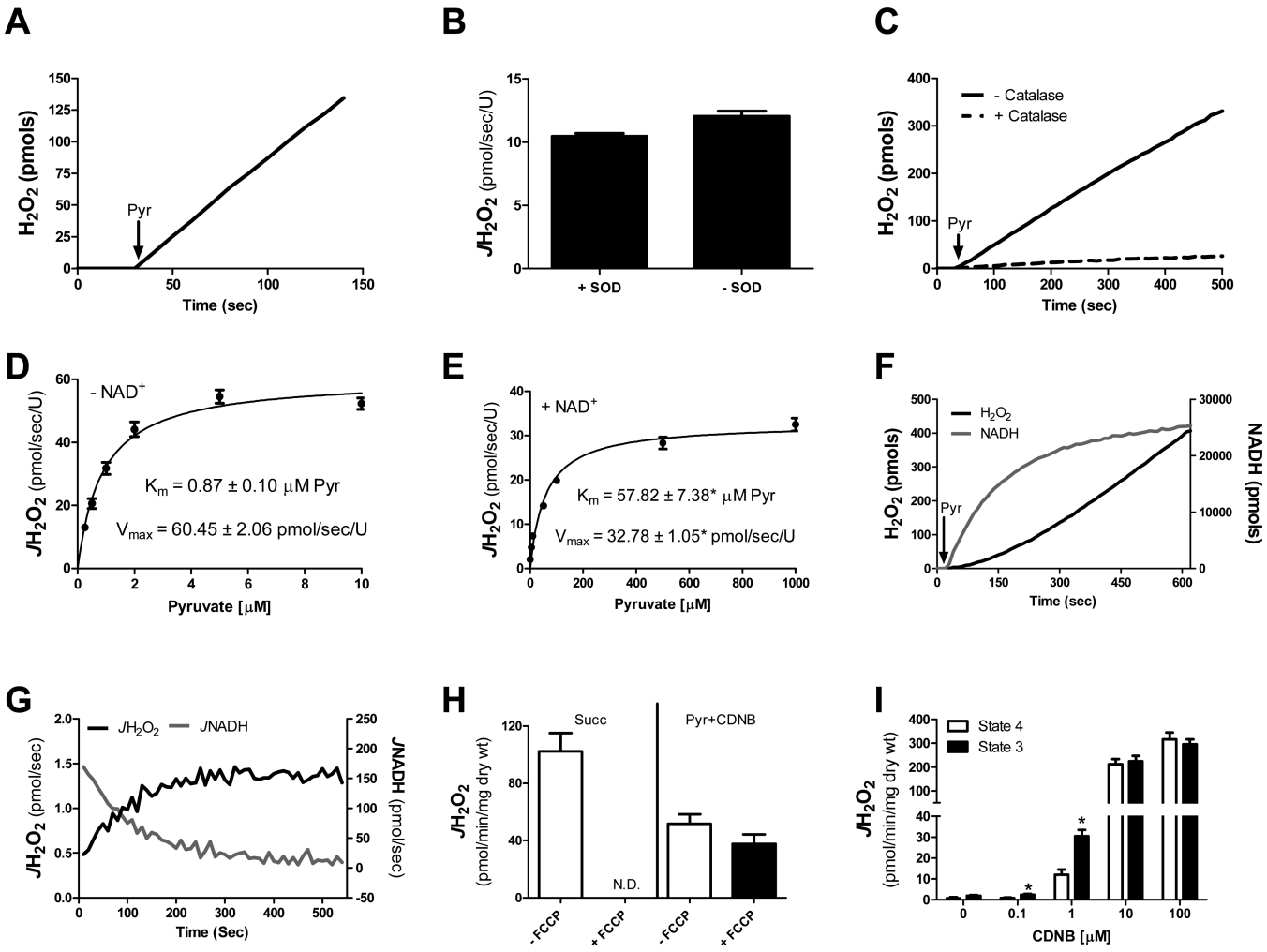

Figure 4. PDC-mediated H_2O_2 production: Effects of NADH/NAD and mitochondrial membrane potential

(**A-G**) Data were generated using PDC from porcine heart. (**A**) Representative H_2O_2 production experiment. Black arrows indicate the addition of pyruvate (1 mM). (**B**) H_2O_2 production in the absence and presence of 25 U/ml SOD. (**C**) H_2O_2 production in the absence and presence of 100 U/ml catalase. For these experiments, HRP was reduced to 100 mU/ml in order to allow catalase to outcompete HRP for any potential H_2O_2. (**D-E**) H_2O_2 production in response to increasing concentrations of pyruvate in the absence (**D**) or presence (**E**) of NAD^+. K_m and V_{max} values (with respect to H_2O_2 production) were calculated using Prism statistical software. *Different from - NAD^+ condition. (**F**) Representative H_2O_2 production (black trace) and NADH production (grey trace) experiment in response to 1 mM pyruvate (50 μM NAD^+ was present for all assays). (**G**) Quantified flux derivative from experiment depicted in panel **F**. JH_2O_2 and JNADH were plotted together (pmol/sec). (**H**) Permeabilized fibers were prepared from RG of C57BL/6NJ mice and pre-treated with 0 or 100 nM CDNB. JH_2O_2 emission was assessed in response to succinate (10 mM) and pyruvate (1 mM) in the absence and presence of FCCP (5 μM). (**I**) Permeabilized fibers were prepared from RG of Sprague Dawley rats and pre-treated with varying concentrations of CDNB. JH_2O_2 emission was assessed in response to pyruvate (1 mM) in the absence (State 4) and presence (State 3) of maximal ADP (2 mM). Data are mean ± SEM, n = 3-4/group (**A-G**), n = 6-8/group (**H-I**).

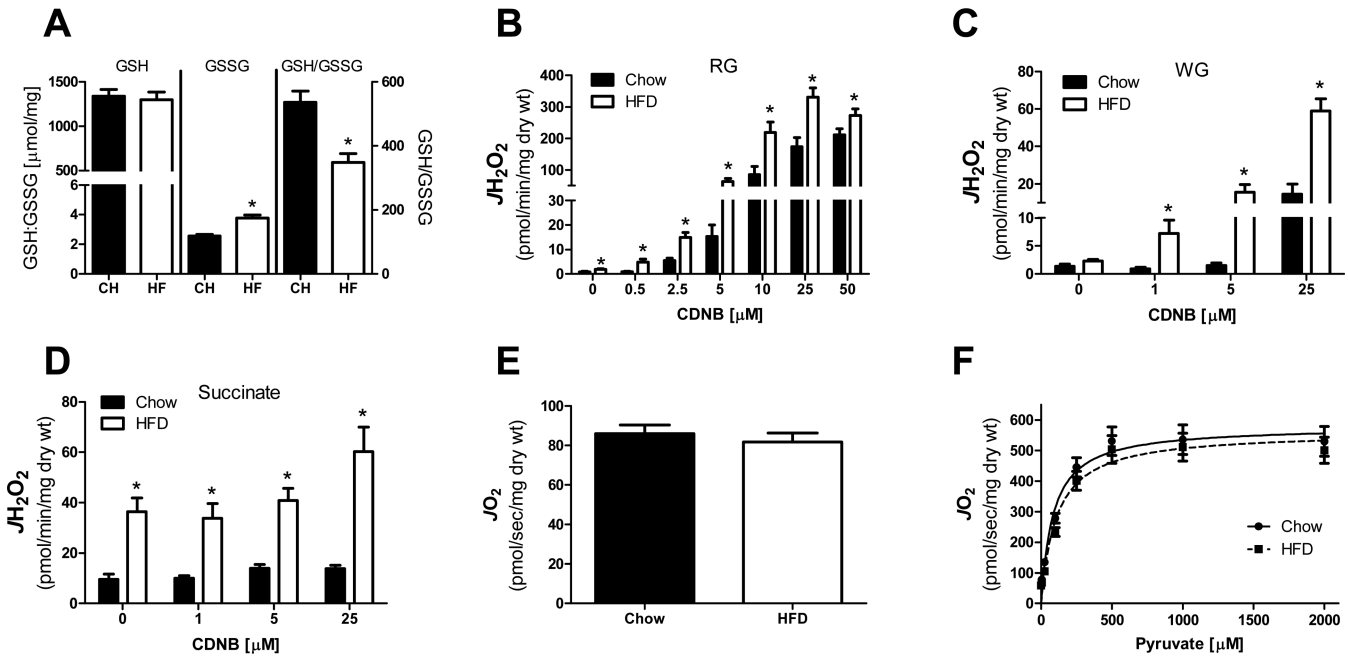

Figure 5. HFD shifts the glutathione redox state to a more oxidized state and elevates pyruvate-supported JH_2O_2 emission within permeabilized myofibers

(**A**) Reduced (GSH) and oxidized (GSSG) glutathione, as well as the ratio of GSH/GSSG were assessed in homogenate prepared from red gastrocnemius muscle. * Different from Chow ($p < 0.05$). (**B-C**) Permeabilized myofibers were prepared from RG or WG of ~18 week old Sprague Dawley rats fed either a 60% High fat or standard chow diet for a period of 6 weeks. Pyruvate (1 mM) supported JH_2O_2 emission was assessed in fibers prepared from RG (**B**) or WG (**C**) muscle and pre-treated with varying concentrations of CDNB. *Different from Chow ($p < 0.05$). (**D**) Succinate (10 mM) supported JH_2O_2 emission was assessed in fibers prepared from RG muscle and pre-treated with varying concentrations of CDNB. *Different from Chow ($p < 0.05$). (**E**) JO_2 consumption in response to pyruvate (1 mM) in the absence of ADP in fibers prepared from RG. (**F**) JO_2 consumption in the presence of malate (2 mM) and ADP (2 mM) in response to increasing concentrations of pyruvate in fibers prepared from RG. Data are mean ± SEM, n = 8-10/group.